



**HAL**  
open science

## Low-frequency noise considerations for sensors based on manganites

Bruno Guillet, Stéphane Flament, Shuang Liu, Olivier Rousseau, Ammar Aryan, Marc Lam Chok Sing, Laurence Méchin, Jean-Marc Routoure, Luiz Guiherme Enger, Sylvain Lebargy, et al.

### ► To cite this version:

Bruno Guillet, Stéphane Flament, Shuang Liu, Olivier Rousseau, Ammar Aryan, et al.. Low-frequency noise considerations for sensors based on manganites. ICNF 2019 (25th International Conference on Noise and Fluctuations), Jun 2019, Neuchatel, Switzerland. pp.326-329, 10.5075/epfl-ICLAB-ICNF-269309 . hal-02336146

**HAL Id: hal-02336146**

**<https://normandie-univ.hal.science/hal-02336146>**

Submitted on 28 Oct 2019

**HAL** is a multi-disciplinary open access archive for the deposit and dissemination of scientific research documents, whether they are published or not. The documents may come from teaching and research institutions in France or abroad, or from public or private research centers.

L'archive ouverte pluridisciplinaire **HAL**, est destinée au dépôt et à la diffusion de documents scientifiques de niveau recherche, publiés ou non, émanant des établissements d'enseignement et de recherche français ou étrangers, des laboratoires publics ou privés.

# Low-frequency noise considerations for sensors based on manganites

Guillet Bruno  
Normandie Univ, UNICAEN,  
ENSICAEN, CNRS, GREYC  
Caen, France  
bruno.guillet@unicaen.fr

Aryan Ammar  
Normandie Univ, UNICAEN,  
ENSICAEN, CNRS, GREYC  
Caen, France  
ammar.aryan@unicaen.fr

Enger Luiz Guilherme  
Normandie Univ, UNICAEN,  
ENSICAEN, CNRS, GREYC  
Caen, France  
luiz-guilherme.enger@ensicaen.fr

Flament Stéphane  
Normandie Univ, UNICAEN,  
ENSICAEN, CNRS, GREYC  
Caen, France  
stephane.flament@ensicaen.fr

Lam Chok Sing Marc  
Normandie Univ, UNICAEN,  
ENSICAEN, CNRS, GREYC  
Caen, France  
marc.lam@ensicaen.fr

Lebargy Sylvain  
Normandie Univ, UNICAEN,  
ENSICAEN, CNRS, GREYC  
Caen, France  
sylvain.lebargy@unicaen.fr

Liu Shuang  
Normandie Univ, UNICAEN,  
ENSICAEN, CNRS, GREYC  
Caen, France  
shuang.liu@unicaen.fr

Méchin Laurence  
Normandie Univ, UNICAEN,  
ENSICAEN, CNRS, GREYC  
Caen, France  
laurence.mechin@ensicaen.fr

Nascimento Vanuza Marques  
Normandie Univ, UNICAEN,  
ENSICAEN, CNRS, GREYC  
Caen, France  
marques-donascimento@unicaen.fr

Rousseau Olivier  
Normandie Univ, UNICAEN,  
ENSICAEN, CNRS, GREYC  
Caen, France  
olivier.rousseau@unicaen.fr

Routoure Jean-Marc  
Normandie Univ, UNICAEN,  
ENSICAEN, CNRS, GREYC  
Caen, France  
jean-marc.routoure@unicaen.fr

Wu Sheng  
Normandie Univ, UNICAEN,  
ENSICAEN, CNRS, GREYC  
Caen, France  
sheng.wu@unicaen.fr

**Abstract**—Low frequency noise considerations for sensors based on  $\text{La}_{0.33}\text{Sr}_{0.67}\text{MnO}_3$  (LSMO) thin films are discussed in this paper. Thanks to special attention on the film quality, on the electrical readout electronics and on the patterned geometries, epitaxially grown LSMO thin films can show a very low level of low-frequency noise and can thus be used to fabricate high signal-to-noise ratio sensors such as uncooled bolometers and uncooled low-field magnetoresistances.

**Keywords**— low frequency noise, LSMO, bolometers, magnetoresistances

## I. INTRODUCTION

Among manganites, the ferromagnetic composition  $\text{La}_{0.33}\text{Sr}_{0.67}\text{MnO}_3$  (LSMO) with a Curie temperature of 360 K is particularly promising for sensors since the metal-to-insulator transition accompanying the ferromagnetic-to-paramagnetic transition occurs above room temperature, thus allowing room temperature applications [1].

The objective of the present paper is to show that before using LSMO thin films for sensors, we had to optimize the deposition conditions, the patterned geometries and the electronic readout in order to obtain very low electrical noise, as summarized in section II. In addition, we show the effect of film thickness on the structural and electrical properties. Section III and section IV briefly present two examples of high signal-to-noise ratio sensors based on LSMO thin films: uncooled bolometers on buffered silicon substrates [2,3], and uncooled low-field magnetic sensors on  $\text{SrTiO}_3$  (STO) substrates [4].

## II. LSMO MATERIAL PROPERTIES AND CONTACT DESIGN

LSMO films of various thicknesses in the 5-150 nm range were epitaxially grown either on STO (100) substrates by Pulsed Laser Deposition (PLD) or on STO buffered Si

(001) substrates by reactive Molecular Beam Epitaxy (MBE) [5].

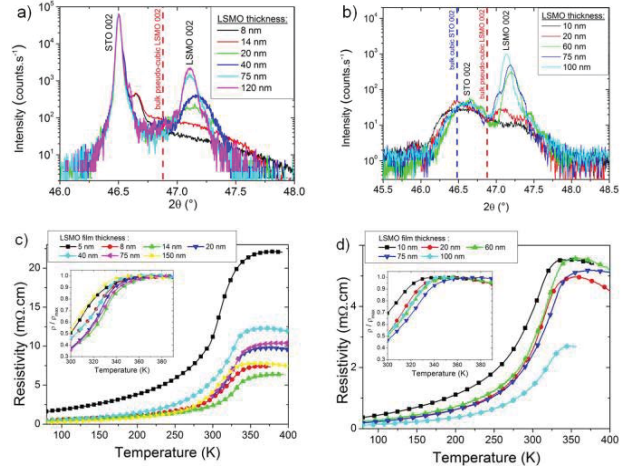


Fig. 1.  $\theta$ - $2\theta$  out-of-plane X-ray Diffraction (XRD) and resistivity versus temperature measurements, respectively, for (a) and (c) LSMO / STO (001); (b) and (d) LSMO/Si (001).

The lattice mismatch between epitaxial films and substrates can significantly influence the electrical and magnetic properties (DC properties, noise level, etc.). The structural and electrical properties were systematically checked using  $\theta$ - $2\theta$  out-of-plane X-ray Diffraction (XRD) and electrical resistivity versus temperature measurements, respectively, as shown in Fig. 1. From the out-of-plane lattice parameter of LSMO, named  $c_{\text{LSMO}}$ , we could measure the LSMO out-of-plane lattice deformation  $\varepsilon_{[001]}$  defined as

$$\varepsilon_{[001]} = (c_{\text{LSMO}} - c_{\text{LSMOpc}}) / c_{\text{LSMOpc}} \quad (1)$$

where  $c_{\text{LSMOpc}}$  is the pseudo-cubic lattice parameter of bulk LSMO (0.3873 nm).  $\varepsilon_{[001]}$  is negative for the whole film thickness range, as expected in case of tensile strain, when grown on STO material, of lattice parameter equal to 0.3905 nm.

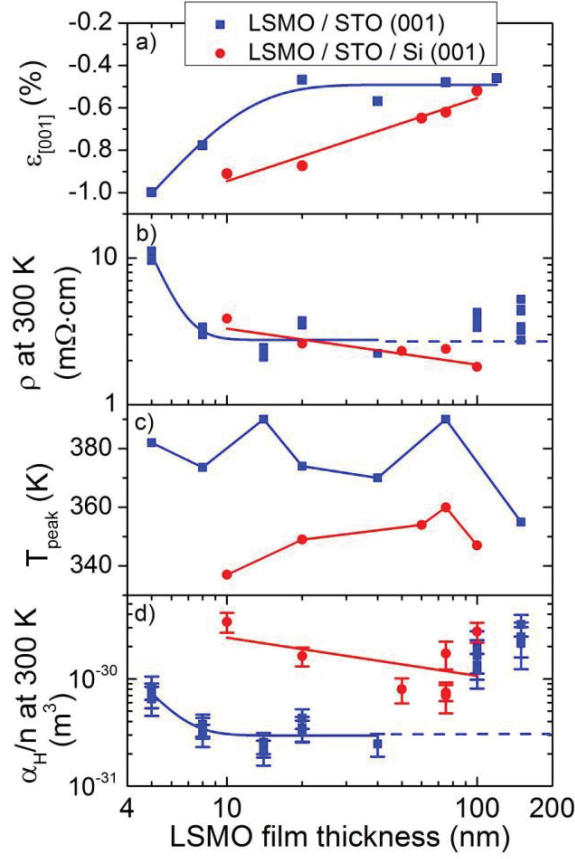


Fig. 2.  $\varepsilon_{[001]}$ , electrical resistivity at 300 K,  $T_{\text{peak}}$  and  $\alpha_H/n$  versus LSMO film thickness in case of STO and STO/Si substrates.

As shown in [6] noise spectra typically consist of two parts: the low-frequency noise that depends on the bias current and the frequency, and the white (or Johnson) noise that is equal to  $4k_bTR$ , where  $k_b$  is the Boltzmann constant,  $T$  is the temperature and  $R$  is the sample electrical resistance. We used the semi-empirical Hooke relation to describe the low frequency noise in our samples [7]:

$$S_V/V^2 = \alpha_H/(n\Omega f) \quad (2)$$

where  $S_V$  is the voltage noise spectral density ( $V^2 \text{ Hz}^{-1}$ ),  $V$  is the sample voltage (V),  $\alpha_H$  is the Hooke parameter (dimensionless),  $n$  is the charge carrier concentration ( $\text{m}^{-3}$ ). The electrical resistivity at 300 K and the temperature  $T_{\text{peak}}$  at which the electrical resistivity is maximum are other parameters of interest.  $\varepsilon_{[001]}$ , the electrical resistivity at 300 K and  $T_{\text{peak}}$  are then plotted in Fig 2.a), b) and c) as a function of film thickness, together with the normalized Hooke parameters  $\alpha_H/n$ , which gives an indication of the 1/f noise level of the material, in Fig 2.d).

In order to measure the low frequency noise, a four-probe configuration was used and home-made electronics was designed. The voltage instrumentation amplifier circuit was build using 3 low noise operational amplifiers AD743,

leading to a noise floor of  $20 \times 10^{-18} \text{ V}^2 \cdot \text{Hz}^{-1}$  in 1 Hz – 100 kHz bandwidth and negligible input current noise. A quasi-ideal DC current source was specifically designed, and showed high output impedance and negligible output current noise [8].

In addition to dedicated low noise electronics, a specific attention has been paid on the electrical contacts [2], as well as on the contact geometry in order to minimize parasitic effects, due to non-homogeneity in the current density distribution. Samples were patterned with different designs. More details will be given in a coming paper. The mask designs are made to avoid any deviation of the current lines. When the geometry is not well chosen, up to 3 orders of magnitude difference in  $\alpha_H/n$  values have been measured on the same sample.

Finally, we showed that a clear correlation exists between the 1/f noise level, the temperature of the metal-to-insulator transition and the thickness of the LSMO thin film as previously published in [9]. In case of well matched crystalline substrate (for example STO), higher noise was measured in films thinner than 10 nm, where higher electrical resistivity and higher lattice deformation were also measured. In the 20 – 80 nm thickness range, LSMO films are very probably relaxed and therefore show low noise values. At about 80 nm, which can be close to the critical thickness value for epitaxial films on STO, one can observe an increase of the noise levels, which can be related to the presence of inhomogeneous strain as stated above, or even cracks for these higher thickness values. On STO/Si substrate, the 1/f noise level can be larger by up to one order of magnitude but stayed at very low values. They do not show a clear dependence versus thickness as it was seen on STO. LSMO films on STO/Si were used for bolometers, in order to allow the use of standard micromachining techniques of silicon. LSMO films on STO were used for anisotropic magnetoresistances. In that case film thickness was kept below 25 nm so as to get a uniaxial magnetic anisotropy [10].

Figure 3 shows the dependence of the normalized Hooke parameters with the electrical resistivity of LSMO thin films of various thicknesses deposited on STO substrates and on buffered Si substrates. The normalized Hooke parameter could be lower than  $10^{-30} \text{ m}^3$  in a large number of cases.

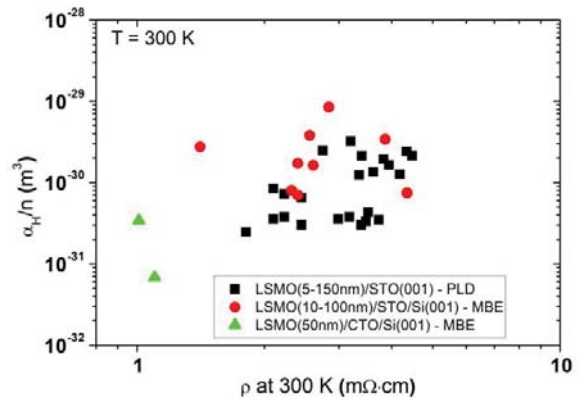


Fig. 3. Correlation between normalised Hooke parameter and electrical resistivity of LSMO thin films of various thicknesses on STO substrates and buffered Si substrates.

### III. PERFORMANCE OF LSMO DEVICES

#### A. LSMO uncooled bolometers

A bolometer measures the power of incident electromagnetic radiation via the heating of a material with a temperature-dependent sensor. The classical principle is based on the variation of a electrical resistance due to absorbed electromagnetic radiation. The bolometers are usually used in infrared radiation measurements since optical responsivity depends on the absorbed wavelength only through absorption. The performance of a bolometer is mainly determined by Temperature Coefficient of Resistance (TCR) and low thermal conduction.

LSMO is a promising candidate for fabricate uncooled bolometers thanks to the large TCR (around 2-3 %  $K^{-1}$ ) close to room temperature and a low-noise level compared with other resistive materials such as semiconductors (a-Si, a-Si:H, a-Ge, poly SiGe) and other oxide materials (semiconducting YBCO,  $VO_x$ , etc.). An example of the electrical resistivity and the derivative of R versus T noted  $dR/dT$  is shown in figure 4.

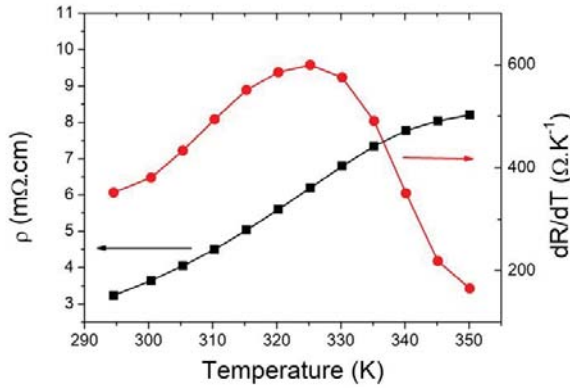


Fig. 4. Electrical resistivity (left axis) and derivative of the electrical resistance (right axis) versus temperature of a suspended 150  $\mu\text{m}$  long and 4  $\mu\text{m}$  wide bridges patterned in a 75 nm thick LSMO thin films.

Non-suspended and free-standing LSMO bolometers have been investigated (Fig. 5) [2,3,11]. The substrate below the active area can be removed by using standard micromachining techniques, which reduce thermal conductance and therefore enables to fabricate sensitive and fast sensors, while keeping very low intrinsic electrical noise. The thermal conductance can be reduced by 3 orders of magnitude (down to  $10^{-7} \text{ W}\cdot\text{K}^{-1}$ ) thus increasing the sensitivity by a factor of 1000.

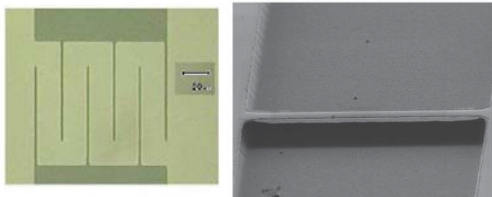


Fig. 5. Examples of non-suspended meander of width 18  $\mu\text{m}$  and free-standing LSMO bolometers of width 4  $\mu\text{m}$  and length 50  $\mu\text{m}$ .

Thanks to the very low  $1/f$  noise, and with appropriate geometries, ultra low Noise Equivalent Power (NEP) values around  $\text{pW}\cdot\text{Hz}^{-1/2}$  could be obtained at 300 K. An example of

an ultra low NEP value is given in Fig. 6 for a phonon noise limited bolometer.

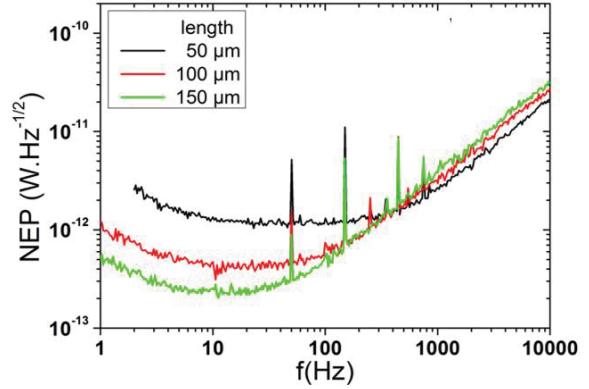


Fig. 6. NEP of a 75 nm thick 2  $\mu\text{m}$  wide suspended bolometer with different length.

#### B. LSMO uncooled low-field magnetoresistances

One major problem with low-field magnetic sensors is their excess noise at low frequency. Therefore, thanks to their low  $1/f$  noise, LSMO may find important applications in magnetoresistive sensors. Moreover, LSMO exhibits a Curie temperature of about 350 K, which allows room temperature applications. An example of measured differential voltage of a Wheatstone bridge patterned in LSMO and relative magnetic field sensitivity as a function of the magnetic field  $\mu_0 H$  are shown in Fig. 7. The observed magnetoresistance is due to anisotropic effect in a ferromagnetic film showing uniaxial anisotropy.

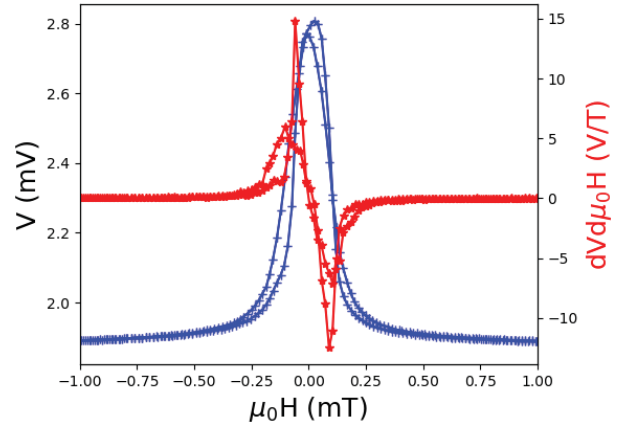


Fig. 7. (left axis) Example of differential voltage of a Wheatstone bridge (current perpendicular to applied magnetic field, bias current = 200  $\mu\text{A}$ ,  $R=8100 \Omega$ ,  $T=310 \text{ K}$ ) showing an uniaxial anisotropy, and (right axis) relative magnetic field sensitivity as a function of the magnetic field  $\mu_0 H$ .

Some growth parameters such as the nature of the substrate, and the direction of the patterned stripes with respect to the easy magnetization axis, were modified in order to optimize the magnetic detectivity of the realized devices. Making use of uniaxial anisotropy in thin LSMO films on STO (001) and the Anisotropic MagnetoResistive effect (AMR), we could measure sensitivity of about  $400\% \cdot T^{-1}$ .

Promising results were obtained on Wheatstone bridge geometries patterned in LSMO thin films. Magnetic noise

was finally measured to be in the order of 200 pT·Hz<sup>-1/2</sup> at 310 K in a frequency range corresponding to neuron activities (Fig. 8).

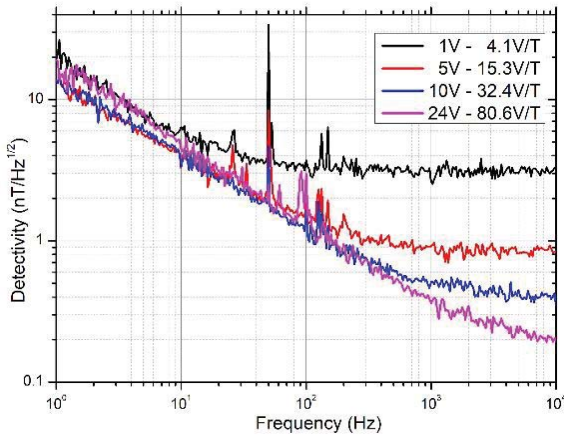


Fig. 8. Example of detectivity versus frequency at 0.2 mT and at different bias voltage (current perpendicular to applied magnetic field,  $R=8100 \Omega$ ,  $T = 310 \text{ K}$ ).

#### IV. CONCLUSIONS

We have shown that LSMO thin films, associated with home-made readout and specific mask design, could be useful to fabricate state of the art uncooled bolometers and magnetoresistances.

#### ACKNOWLEDGMENT

This project has received funding from the European Union's Horizon 2020 research and innovation programme under grant agreement No. 737116 (byAxon)

#### REFERENCES

- [1] Coll M. *et al.*, "Towards Oxide Electronics: A Roadmap", *Appl. Surf. Science*, 482, 1-93, 2019
- [2] Liu S., Guillet B., Aryan A., Adamo C., Fur C., Routoure J.M., Lemarié F., Schlom D.G., Méchin L., "La<sub>0.7</sub>Sr<sub>0.3</sub>MnO<sub>3</sub> suspended microbridges for uncooled bolometers made using reactive ion etching of the silicon substrates", *Microelec. Eng.*, 111 101-104, 2013
- [3] Liu. S., Guillet B., Adamo C., Nascimento V.M., Lebargy S., Brasse G., Lemarié F., El Fallah J., Schlom D.G. and Méchin L., "Free-standing La<sub>0.7</sub>Sr<sub>0.3</sub>MnO<sub>3</sub> suspended micro-bridges on buffered silicon substrates showing undegraded low frequency noise properties", *J. Micromech. Microeng.*, 29, 6, 065008, 2019
- [4] Perna P., Maccariello D., Ajejas F., Guerrero R., Méchin L., Flament S., Santamaria J., Miranda R. and Camarero J., "Large Anisotropic Magnetoresistance in La<sub>0.7</sub>Sr<sub>0.3</sub>MnO<sub>3</sub> Films at Room Temperature", *Adv. Func. Mat.*, 1700664, 2017
- [5] Méchin L., Adamo C., Wu S., Guillet B., Lebargy S., Fur C., Routoure J.-M., Mercone S., Belmeguenai M. and Schlom D.G., "Epitaxial La<sub>0.7</sub>Sr<sub>0.3</sub>MnO<sub>3</sub> Thin Films Grown on SrTiO<sub>3</sub> Buffered Silicon Substrates by Reactive Molecular-Beam-Epitaxy", *Phys. Status Solidi A*, 209, 1090, 2012
- [6] Méchin L., Routoure J.-M., Mercone S., Yang F., Flament S. and Chakalov R.A., "1/f noise in patterned La<sub>2/3</sub>Sr<sub>1/3</sub>MnO<sub>3</sub> thin films in the 300–400K range", *J. Appl. Phys.*, 103, 083709, 2008
- [7] Hooge F.N., "1/f noise is no surface effect", *Phys. Lett.*, 29A, 139, 1969
- [8] Routoure J.M., Wu S., Barone C., Mechin L., Guillet B., "A Low-Noise and Quasi-Ideal DC Current Source Dedicated to Four-Probe

Low-Frequency Noise Measurements", *IEEE Trans. Instrum. Meas.*, DOI: 10.1109/TIM.2019.2890891, 2019

- [9] Mechin L., Wu S., Guillet B., Perna P., Fur C., Lebargy S., Adamo C., Schlom D.G. and Routoure J.-M., "Experimental evidence of correlation between 1/f noise level and metal-to-insulator transition temperature in epitaxial La<sub>0.7</sub>Sr<sub>0.3</sub>MnO<sub>3</sub> thin films", *J. Phys. D: Appl. Phys.*, 46, 202001, 2013
- [10] Chaluvadi S.K., Perna P., Ajejas F., Camarero J., Pautrat A., Flament S., and Méchin L., "Thickness and angular dependent magnetic anisotropy of La<sub>0.67</sub>Sr<sub>0.33</sub>MnO<sub>3</sub> thin films by vectorial magneto optical kerr magnetometry", *IOP Conf. Series: Journal of Physics: Conference Series (JPCS)*, 903 012021, 2017
- [11] Aryan A., Guillet B., Routoure J.M., Fur C., Langlois P., Méchin L., "Measurement of thermal conductance of La<sub>0.7</sub>Sr<sub>0.3</sub>MnO<sub>3</sub> thin films deposited on SrTiO<sub>3</sub> and MgO substrates", *Appl. Surf. Science*, 326, 204, 2015